Transition moments for energy transfers in Ar-Cl$^+$ collisions

Douglas A. Chapman, K. Balasubramanian, and S. H. Lin

Department of Chemistry, Arizona State University, Tempe, Arizona 85287-1604

Joyce J. Kaufman, P. C. Hariharan, and W. S. Koski

Department of Chemistry, The Johns Hopkins University, Baltimore, Maryland 21218

(Received 22 November 1988)

Relativistic configuration-interaction calculations are carried out including the spin-orbit term for the transition moments for energy transfers in Ar-Cl$^+$ collisions. Our calculations indicate that once the bound $^1\Sigma^+$ state of ArCl$^+$ is formed through Ar($^1S_0$)+Cl$^+$($^1D_2$) collisions, the transition moment for the $^1\Sigma^+$ state to dissociate into ground-state species is so small that ArCl$^+$ would be long lived in the $^1\Sigma^+$ state. This is consistent with the experimental findings.

I. INTRODUCTION

Recently, transitions between the ^3P and ^1D terms of Cl$^+$ were observed in inelastic collisions between Cl$^+$ and Ar.[1] The collision-induced energy-transfer processes were examined in the context of a Landau-Zener model, whereby energy transfer between colliding species takes place at the points of intersection of the rare-gas–halogen-ion intermediate complex. Complete active space self-consistent-field (CASSCF)/first-order configuration-interaction (FOCI) potential curves were also reported for electronic states of ArCl$^+$ associated with the Ar(^1S)+Cl$^+$(^3P), Ar(^1S) +Cl$^+$(^1D), and Ar$^+$(^2P) +Cl(^2P) asymptotes.[1] The existence of a trio of bound electronic states ($^3\Pi$, $^1\Sigma^+$, $^1\Pi$) correlating into the Ar(^1S)+Cl$^+$(^3P, ^1D) limits was predicted by these calculations.

An experimental D_e value for ArCl$^+$ of 1.75 eV has been inferred by Sharma and Koski[2] through collision-induced dissociation of ArCl$^+$ in Ar. The theoretical CASSCF/FOCI D_e value[1] for the excited $^1\Sigma^+$ state of ArCl$^+$, 1.85 eV, is in excellent agreement with the experimental value, implying that the $^1\Sigma^+$ state of ArCl$^+$, formed by collisions between Ar(^1S) and Cl$^+$(^1D), should be a relatively stable, long-lived entity. However, a mechanism for the formation of this state has not been presented to date. Further, many curve crossings arise among the λ-s states (states obtained using the λ-s scheme without spin-orbit interaction) of ArCl$^+$ which could significantly impact energy transfers between the colliding species, as well as the radiative lifetimes of the resulting intermediate complex. Experimentally, ArCl$^+$ has been found to be a long-lived species. There are no satisfactory explanations as to why ArCl$^+$ is so long lived considering the crossings of the repulsive $^3\Sigma^-$ curve and the repulsive wall of the $^3\Pi$ curve with the $^1\Sigma^+$ state near the bottom of the well. Thus, the purpose of this article is to present electronic transition moments and potential curves constructed in an intermediate-coupled relativistic CI (RCI) formalism. In the RCI method, different λ-s states which give rise to states of the same Ω($\Omega=\lambda+s$) symmetry are mixed in a variational manner in the pres-

ence of the spin-orbit operator. These data are then utilized in an effort to resolve the kinetic-energy spectra[1] resulting from collisions of Cl$^+$ with Ar. Electronic transition moments are calculated in the neighborhood of points of intersection of the ArCl$^+$ potential curves in order to examine mechanisms by which ArCl$^+$, once formed, could become a stable species. Quantitative Mulliken population analyses are also utilized to explain the calculated transition moments.

II. EXPERIMENTAL METHODS AND RESULTS

A. Energy-transfer experiments

The techniques utilized to study collisions of Cl$^+$ with Ar in a tandem mass spectrometer have been previously described.[1-3] The beam composition of Cl$^+$ was found to be 60% Cl$^+$ ($^3P_{0,1,2}$) and 40% Cl$^+$ ($^1D_2$) as determined by an attenuation method. In summary, the experimental method proceeds as follows: a monoenergetic ion beam of Cl$^+$ (0.1 eV FWHM) was passed through a shallow reaction chamber containing the target gas Ar at pressures of 10^{-4} Torr. Under these conditions, observations are made under single binary collision conditions. The ions scattered at 0° relative to the primary-ion beam direction were then mass analyzed by a second quadrupole mass filter, energy analyzed by an electrostatic analyzer, and detected with an electron multiplier.

The kinetic-energy spectrum obtained in this way is shown in Fig. 1 of Ref. 1. Basically, the spectrum consists of a "superelastic" peak spaced at 1.38 eV relative to the unperturbed Cl$^+$ peak, and a "subelastic" peak shifted to -1.42 eV relative to the 0 eV Cl$^+$ peak. The peaks correspond to transitions between the $^1D_2$ and $^3P_{0,1,2}$ terms of Cl$^+$. The superelastic peak at 1.38 eV was thus attributed to the transition Cl$^+$($^1D_2$)$\rightarrow$Cl$^+$($^3P_{0,1,2}$), while the subelastic peak (-1.42 eV) was attributed to the Cl$^+$($^3P_{0,1,2}$)$\rightarrow$Cl$^+$($^1D_2$) transition. It is noted that the spin-orbit splitting among the Cl$^+$ ^3P terms was too small to be resolved by the experimental apparatus.

B. Preparation of $ArCl^+$

$ArCl^+$ was prepared by bombarding a 50% mixture of Ar and Cl_2 at a pressure of 2 Torr. At such pressures, numerous collisions are possible; however, if Ar and Cl^+ collide, they can be stabilized by three-body collisions to yield $ArCl^+$. If the resulting $ArCl^+$ ions are collided with Ar, a collision dissociation reaction such as

$$ArCl^+ + Ar \rightarrow Ar + Ar + Cl^+ \qquad (1)$$

may be observed. This process is endothermic; hence, it may be studied as a function of energy to yield the threshold value for Cl^+ production and, as a result, the heat of formation and bond energy of $ArCl^+$.

III. METHOD OF CALCULATION

We employ Slater-type basis functions for both Ar and Cl. A valence-level triple-ζ basis set described previously in Ref. 4 for Cl is used in the present investigation. For Ar, a basis set described earlier for Kr (Ref. 5) with lower principal quantum number is employed.

The orbital space for the RCI calculations was generated by an SCF calculation which included averaged relativistic effective potentials (REP) for both Ar and Cl as in the previous investigation.[1] The $s^2 p^6$ valence shell of Ar and the $s^2 p^4$ shell of Cl^+ were explicitly retained at the SCF stage. In this way, an orbital space for the ground $^3\Pi$ state of $ArCl^+$ was generated for internuclear distances of 3.75–12.00 bohr.

The RCI calculations in this work are a multireference single and double CIs based on the technique described in Ref. 6. The RCI calculations were carried out using Balasubramanian's modified and enhanced version of the codes based on Ref. 6. The configurations used to construct the reference lists for the $\Omega = 0^+$, 0^-, 1, and 2 spaces of $ArCl^+$ are the same as those shown for $KrBr^+$ in Ref. 5. Although the dimensions of the reference lists are identical for this calculation and Ref. 5, much more extensive excitations from these references were allowed in the present work; hence, the CI spaces are much larger than those shown in Ref. 5. The RCI calculations for $ArCl^+$ included 14 000–17 000 configurations.

IV. RESULTS AND DISCUSSION

Shown in Fig. 1 are the RCI potential curves for the ω-ω states (states which include the spin-orbit term) of $ArCl^+$ which correlate with the $^1D_2(Cl^+) + {}^1S_0(Ar)$ and $^3P_{0,1,2}(Cl^+) + {}^1S_0(Ar)$ terms; Fig. 2 shows the corresponding λ-s curves in the absence of spin-orbit coupling. The dissociation relationships and calculated spin-orbit splittings for the Cl^+ terms obtained in this work are shown in Table I. The calculated splittings were obtained as asymptotic energy differences at 12.00 bohr. As may be seen from Table I, the agreement between theory and experiment for the spin-orbit splittings of ^3P Cl^+ is very good, although the $^1D_2$ asymptote is somewhat higher than the experimental value. It seems that the main reason for the higher separation of the $^1D_2$ state is electron correlation, although it must be noted that our basis
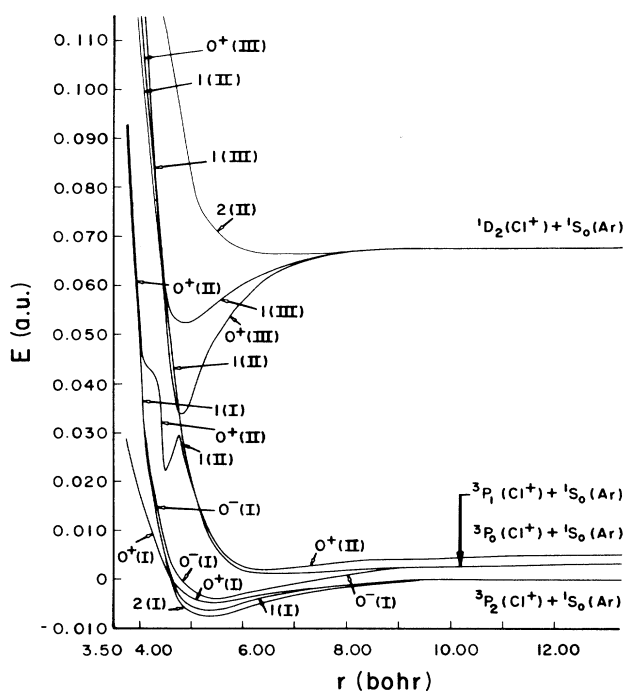

FIG. 1. RCI potential curves for low-lying ω-ω states of $ArCl^+$.

set was optimized for the ground state. Spectroscopic constants for the bound λ-s states ($^3\Pi$, $^1\Sigma^+$, $^1\Pi$) of $ArCl^+$ were previously reported from more accurate CASSCF/FOCI results;[1] also reported in these calculations were spin-orbit corrections for bond lengths and vibrational frequencies for the Ω components of the $^3\Pi$ and
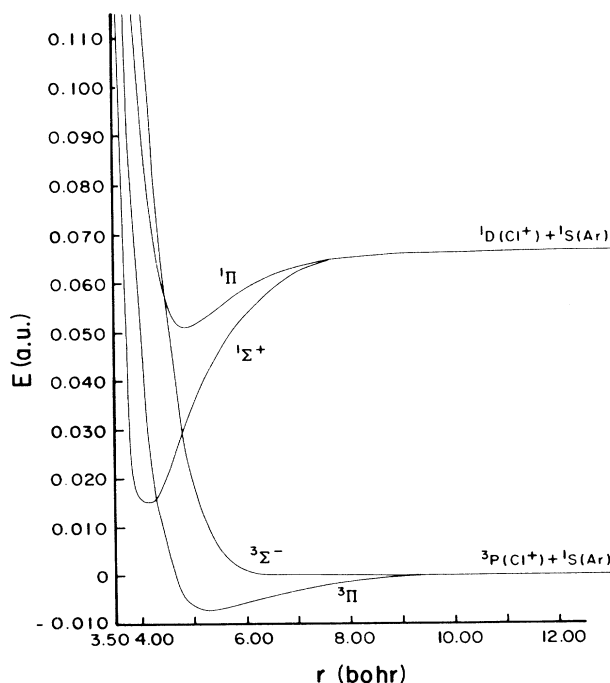

FIG. 2. Potential-energy curves of $ArCl^+$ in the absence of spin-orbit coupling.

TABLE I. Dissociation relationships, theoretical and experimental atomic-energy separations.

Molecular states	Atomic states $Ar + Cl^+$	Energy of the atoms (cm^{-1}) Theory	Expt. (Ref. 7)
$2(I), 0^+(I), 1(I)$	$^1S_0 + {}^3P_2$	0.0	0.0
$1(II), 0^-(I)$	$^1S_0 + {}^3P_1$	665	667
$0^+(II)$	$^1S_0 + {}^3P_0$	1009	996
$0^+(III), 1(III), 2(II)$	$^1S_0 + {}^1D_2$	14789	11652

$^3\Sigma^-$ states of $ArCl^+$.

As may be seen from Fig. 1, the ground $^3\Pi_2 [2(I)]$ state of $ArCl^+$ is slightly bound relative to the $^3P_2(Cl^+) + {}^1S_0(Ar)$ limit. The 1(III) and 0^+(III) states, which correlate into the $^1\Pi$ and $^1\Sigma^+$ λ-s states, respectively, in the absence of spin-orbit terms are much more strongly bound relative to the $^1D_2(Cl^+) + {}^1S_0(Ar)$ asymptote. The 0^+(II) state, which arises as the $\Omega = 0^+$ component of the repulsive $^3\Sigma^-$ state, is seen to exhibit a shallow minimum near 4.50 bohr; this is due to an avoided crossings between the $^3\Pi$ ($\sigma^2\sigma^*\pi^{*3}$) and $^1\Sigma^+$ ($\sigma^2\pi^{*4}$) states at this distance.

Most of the avoided crossings in the various Ω states can be understood if one looks at the curves in Fig. 2 in the absence of spin-orbit coupling. For example, as seen in Fig. 2, the $^3\Pi$ curve crosses with $^1\Sigma^+$. This would lead to an avoided crossing of the corresponding 0^+ components. In the same way, crossing of $^3\Sigma^-$ with $^1\Sigma^+$ leads to avoided crossing of the 0^+ components. The crossing of $^1\Pi$ with $^3\Sigma^-$ results in the avoided crossing of the corresponding 1 components. These avoided crossings are responsible for the unusual shapes of the potential-energy curves in Fig. 1.

As Fig. 1 shows, the 1(II) curve intersects the 0^+(II) curve near 5.00 bohr; the 1(II) curve crosses the 0^+(III) surface at shorter distances (4.75 bohr). The 1(II) state correlates asymptotically to the $^3P_1$ term of Cl^+, while the 0^+(II) and 0^+(III) states dissociate to $^3P_0$ and $^1D_2(Cl^+)$, respectively. According to the Landau-Zener model, the energy transfer between colliding species occurs most efficiently at points where the electronic-state potential curves of the intermediate complex intersect. Thus, the 0^+(III)–1(II) curve crossing at 4.75 bohr would provide a channel by which the $^1D_2 \rightleftarrows {}^3P_1$ transition of Cl^+ could be observed. It is noted that, in Fig. 1, the potential curves associated with the $^3P_2$ term of Cl^+ do not intersect the curves which dissociate to $^1D_2(Cl^+)$; hence, there does not appear to be an available channel by which the $^1D_2 \rightleftarrows {}^3P_2$ transition of Cl^+ could be observed. Thus, it may be concluded that the peaks observed in the kinetic-energy spectra[1] of Cl^+ resulting from the Ar-Cl^+ collisions are due to the transitions Cl^+ ($^3P_{0,1} \rightleftarrows {}^1D_2$), although, as mentioned, the spin-orbit splittings among the ^3P terms of Cl^+ were too small to be resolved by the experimental apparatus.

As seen from Figs. 1 and 2, although the $^1\Sigma_0^+$ $[0^+$(III)] state is well bound, the crossing of the 1(II) state near the bottom of the 0^+(III) state could provide a channel for the dissociation of the $^1\Sigma^+$ state. If this transition mo-

ment is, indeed, large, then the $ArCl^+$ ion would not be long lived. While the previous investigation[1] provided for curve crossings and potential-energy curves, the transition moments at curve crossings were not reported. Thus, it was decided to compute transition moments for the various curve crossings.

Electronic transition moments were calculated from the RCI wave functions for the 0^+(II)$\rightarrow$1(II) and 0^+(III)$\rightarrow$1(II) transitions at and near the curve crossings of these states. These data are shown in Table II. Table III shows the weights of the various λ-s states in the RCI wave functions of the 0^+ states. As may be seen in Table II, the transition moments are, in general, quite small in the neighborhood of the curve crossings. This finding seems to be consistent with the experimental observation that the cross sections for the reactions

$$Cl^+({}^1D_2) + Ar \rightleftarrows Cl^+({}^3P_{0,1,2}) + Ar^* \qquad (2)$$
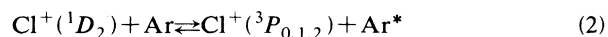
are also small ($10^{-2} - 10^{-3}$ Å^2). It is noted, however, that an observable number of such transitions do occur.

The behavior of the electronic transition moments may be explained by examining the makeup of the RCI wave functions (see Table III) and Mulliken population analysis. At all internuclear distances (see Fig. 2) to the left of 6.00 bohr, the 1(II) state (not shown in Table III) is dominantly ($> 96\%$) of $^3\Sigma^-$ ($\sigma^2\sigma^{*2}\pi^{*2}$) character; at distances longer than 6.00 bohr, significant mixing with $^3\Pi$ ($\sigma^2\sigma^*\pi^{*3}$) is observed in the 1(II) wave function so that it would dissociate into $Cl^+({}^3P_1) + Ar({}^1S_0)$. Near the 0^+(II)–1(II) curve crossing (5.00 bohr), the 0^+(II) state is 96% $^3\Sigma^-$ ($\sigma^2\sigma^{*2}\pi^{*2}$); thus, the 0^+(II) and 1(II) wave functions at 5.00 bohr are dominated by different spin components which arise from the same $^3\Sigma^-$ state, and the 0^+(II)$\rightarrow$1(II) transition probability is very small at the curve intersection as a result.

Avoided crossings in the $ArCl^+$ 0^+(III) wave function play a key role in determining the magnitude of the 0^+(III)–1(II) transition moment, and hence, the radiative lifetime of $ArCl^+$. In the absence of spin-orbit terms the 0^+(III) curve would correlate into the $^1\Sigma^+$ state; however, near the crossing of the 0^+(III) and 1(II) curves (4.75 bohr), the 0^+(III) wave function is predominantly of $^3\Sigma^-$ ($\sigma^2\sigma^{*2}\pi^{*2}$) character; at this same distance, the 1(II) wave function is also dominated by $^3\Sigma^-$ from the same configuration; again, the transition moment is small in magnitude at the curve crossing since the wave functions are dominated by different spin components $[0^+: (1/\sqrt{2})$

TABLE II. RCI electronic transition moments for the 0^+(II)$\rightarrow$1(II) and 0^+(III)$\rightarrow$1(II) transitions of $ArCl^+$. The asterisks denote the potential curve-crossing points. $x[-y]$ denotes $x \times 10^{-y}$.

	Transition moment, Debye	
r (bohr)	0^+(II)$\rightarrow$1(II)	0^+(III)$\rightarrow$1(II)
4.50	$1.38[-2]$	$3.98[-4]$
4.75	$9.97[-5]$	$2.23[-3]^*$
5.00	$2.50[-4]^*$	$8.07[-4]$
5.25	$4.90[-5]$	$8.15[-4]$
5.50	$1.31[-4]$	$5.23[-4]$

TABLE III. Contributions (%) of λ-s states into the 0^+ states of $ArCl^+$. Only the p electrons of Ar and Cl^+ are shown.

r (bohr)	0^+(I)	0^+(II)	0^+(III)
4.00	94 $^1\Sigma^+(\sigma^2\pi^{*4})$	97 $^3\Pi(\sigma^2\sigma^*\pi^{*3})$	92 $^3\Sigma^-(\sigma^2\sigma^{*2}\pi^{*2})$
4.50	95 $^3\Pi(\sigma^2\sigma^*\pi^{*3})$	90 $^1\Sigma^+(\sigma^2\pi^{*4})$	95 $^3\Sigma^-(\sigma^2\sigma^{*2}\pi^{*2})$
4.75	96 $^3\Pi(\sigma^2\sigma^*\pi^{*3})$	85 $^1\Sigma^+(\sigma^2\pi^{*4})$	96 $^3\Sigma^-(\sigma^2\sigma^{*2}\pi^{*2})$
		7 $^1\Sigma^+(\sigma^{*2}\pi^{*4})$	
		4 $^3\Sigma^-(\sigma^2\sigma^{*2}\pi^{*2})$	
5.00	97 $^3\Pi(\sigma^2\sigma^*\pi^{*3})$	96 $^3\Sigma^-(\sigma^2\sigma^{*2}\pi^{*2})$	86 $^1\Sigma^+(\sigma^2\pi^{*4})$
			11 $^1\Sigma^+(\sigma^{*2}\pi^{*4})$
6.00	83 $^3\Pi(\sigma^2\sigma^*\pi^{*3})$	83 $^3\Sigma^-(\sigma^2\sigma^{*2}\pi^{*2})$	70 $^1\Sigma^+(\sigma^2\pi^{*4})$
	15 $^3\Sigma^-(\sigma^2\sigma^{*2}\pi^{*2})$	12 $^3\Pi(\sigma^2\sigma^*\pi^{*3})$	27 $^1\Sigma^+(\sigma^2\sigma^{*2}\pi^{*2})$
9.00	56 $^3\Sigma^-(\sigma^2\sigma^{*2}\pi^{*2})$	55 $^3\Pi(\sigma^2\sigma^*\pi^{*3})$	76 $^1\Sigma^+(\sigma^2\sigma^{*2}\pi^{*2})$
	42 $^3\Pi(\sigma^2\sigma^*\pi^{*3})$	43 $^3\Sigma^-(\sigma^2\sigma^{*2}\pi^{*2})$	22 $^1\Sigma^+(\sigma^2\pi^{*4})$

$(\pi_x^*\alpha\pi_y^*\beta+\pi_x^*\beta\pi_y^*\alpha)$; 1: $\pi_x^*\alpha\pi_y^*\alpha)]$ of the same $^3\Sigma^-$ state. At slightly longer distance (5.0 bohr) the 0^+(III) state becomes purely $^1\Sigma^+$. As seen in Table II even at 5.0 bohr the transition moment is considerably small. Thus on either side of the potential well of the 0^+(III) state, the transition moments are small. Consequently, it would appear that a relatively stable $ArCl^+$ species could be produced by a reaction of the type

$$Ar + Cl^+(^1D) \rightleftharpoons ArCl^+ , \qquad (3)$$

followed by collisional stabilization. If, for instance, the intermediate species formed in this way followed the 0^+(III) curve shown in Fig. 1, then this species could have a reasonably long radiative lifetime, as judged from the small magnitude of the 0^+(III)–1(II) transition moment not only at the curve crossings at other distances as well (Table II).

The small transition probabilities for energy transfers can be explained based on Mulliken population analysis as well, although Mulliken populations cannot be used in an absolute sense due to the way the populations are partitioned and the possibility of basis set superposition errors. In an earlier investigation, the Mulliken population analysis was carried out on all of the low-lying states of $ArCl^+$ (Table IV of Ref. 1). The $^3\Pi$ and $^3\Sigma^-$ states were found to have total gross Ar and Cl populations of 7.8–8.0 and 6.2–6.0, respectively. In these states, the positive charge resides predominantly on the chlorine atom. The bound $^1\Sigma^+$ and $^1\Pi$ states, on the other hand, have gross Ar and Cl populations of 7.5–7.6 and 6.5 and 6.4, respectively. Thus, the positive charge appears to be equally shared between Ar and Cl in the $^1\Sigma^+$ and $^3\Pi$

states. Although the $^3\Pi$ and $^3\Sigma^-$ curves cross the $^1\Sigma^+$ state ($^3\Pi$ crossing closer to the r_e of $^1\Sigma^+$), in order to induce a transition between $^1\Sigma^+$ and $^3\Pi$ or $^3\Sigma^-$, half of the positive charge would have to move from Ar to Cl (or half an electron from Cl to Ar). This charge-transfer process seems to be somewhat less probable even in ω-ω coupling. Thus, once $ArCl^+$ is formed in the $^1\Sigma^+$ state through $Ar(^1S_0) + Cl^+(^1D_2)$ collisions, it seems to be long lived in this state. Consequently, it appears that if all Cl^+ ions are quenched to the $^3P_{0,1,2}$ ground state then the probability of forming long-lived $ArCl^+$ ion may be small.

V. CONCLUSION

Relativistic CI calculations have been carried out on the low-lying ω-ω states of $ArCl^+$. The transition moments in the region of curve crossings were obtained to explain the lifetime of the bound $^1\Sigma^+$ state. Mechanisms whereby the $^3P_{0,1} \rightleftharpoons ^1D_2$ transitions of Cl^+ could occur were addressed, and no evidence for the $^3P_2 \rightleftharpoons ^1D_2$ transition of Cl^+ was found. Transition moments for the transition between the $ArCl^+$ 0^+(III) and 1(II) states were found to be small, confirming the conclusion that $ArCl^+$ in the 0^+(III) state should be a long-lived species with regard to radiative processes.

[1]K. Balasubramanian, P. Feng, J. J. Kaufman, P. C. Hariharan, and W. S. Koski, Phys. Rev. A **37**, 3204 (1988).

[2]R. B. Sharma and W. S. Koski (unpublished).

[3]K. Wendell, C. A. Jones, J. J. Kaufman, and W. S. Koski, J. Chem. Phys. **63**, 750 (1975).

[4]M. Krauss, W. J. Stevens, and P. S. Julienne, J. Comput. Chem. **3**, 372 (1982).

[5]K. Balasubramanian, J. J. Kaufman, P. C. Hariharan, and W. S. Koski, Chem. Phys. Lett. **129**, 165 (1986).

[6]P. A. Christiansen, K. Balasubramanian, and K. S. Pitzer, J. Chem. Phys. **76**, 5087 (1982).

[7]C. E. Moore, *Tables of Atomic Energy Levels*, Natl. Bur. Stand. (U.S.) Circ. No. 467 (U.S. GPO, Washington, D.C., 1971).